Targeting of mixed sequence double-stranded DNA using pyrene-functionalized 2′-amino-α-L-LNA†

Patrick J. Hrdlicka, T. Santhosh Kumar and Jesper Wengel*

Received (in Cambridge, UK) 17th May 2005, Accepted 15th June 2005
First published as an Advance Article on the web 21st July 2005
DOI: 10.1039/b506986f

Incorporation of a single pyrene-functionalized 2′-amino-α-L-LNA monomer X into short DNA strands induces extraordinarily high binding affinity towards complementary DNA (up to 16 °C increase per modification), whereas labile duplexes, suitable as probes for targeting of double stranded DNA, are formed upon positioning of two monomers X in an interstrand +1 zipper motif.

Development of small molecules that enable sequence-selective targeting of double-stranded DNA (dsDNA) has been stimulated by their potential applications as biomolecular tools within nucleic acid diagnostics or as therapeutics. Progress within this field has been accomplished with minor groove binding polyamides,[1] with DNA triple-helix-based approaches using modified oligonucleotides[2] or helix-invading peptide nucleic acids (PNAs)[3] or with pseudo-complementary DNA (pcDNA)[4–6] or pcPNA.[6,7] However, the full potential of dsDNA targeting by the above mentioned strategies has not been attained due to target sequence restrictions,[1–3] requirements for highly modified probes,[4–7] the necessity for non-physiological salt concentrations[8] or self-inhibitory effects at the high probe concentrations necessary to effect strand invasion.[9] Development of alternative strategies for the targeting of mixed sequence dsDNA at physiologically relevant salt concentrations is therefore highly desirable.

The high-affinity hybridizations of LNA,[10–12] 2′-amino-LNA[13] and α-L-LNA[14] towards complementary DNA and RNA sequences are well established, and have stimulated the development of N2′-functionalized 2′-amino-LNA building blocks.[15–17] Using these building blocks, we have demonstrated that precise positioning of chemical entities in the minor groove of nucleic acid duplexes may result in nucleic acid architectures with potential applications within Ångström-scale chemical engineering.[18]

Herein, we report the synthesis, thermal denaturation experiments and fluorescence properties of oligodeoxyribonucleotides (ONs) containing the first N2′-functionalized derivative of a new class of locked nucleic acids, 2′-amino-α-L-LNAs,[19] and introduce their use as probes for targeting dsDNA.

Nucleic Acid Center‡, Department of Chemistry, University of Southern Denmark, DK-5230 Odense M, Denmark. E-mail: jwe@chem.sdu.dk; Fax: (+45) 6615 8780; Tel: (+45) 6550 2510

† Electronic supplementary information (ESI) available: discussion regarding synthesis of nucleosides **1**–**3** and **ON1**–**ON7**, details of thermal denaturation, fluorescence, dsDNA recognition and molecular modelling experiments, absorption maxima of oligonucleotides (Table S1), lowest energy structure of **ON4**:**ON7** from molecular modelling (Fig. S1) and additional steady-state fluorescence emission spectra of molecular recognition experiments (Fig. S2). See http://dx.doi.org/10.1039/b506986f

‡ A research center funded by the Danish National Research Foundation for studies on nucleic acid chemical biology.

The effect on duplex stability upon incorporation of 2′-*N*-(pyren-1-yl)methyl-2′-amino-α-L-LNA monomer **X** into ONs was evaluated by UV thermal denaturation experiments using medium salt buffer ([Na^+] = 110 mM)† and compared to the corresponding unmodified reference duplexes (Table 1). In all cases the denaturation curves displayed sigmoidal monophasic transitions with a shape similar to that observed for unmodified reference duplexes. Introduction of a single monomer **X** in mixed sequence 9-mer ONs induces extraordinary increases in duplex stability towards complementary DNA (ΔT_m = +7.0 to +16.0 °C relative to unmodified reference duplex **ON1**:**ON2**). Slightly lower stabilization is observed upon incorporation of monomer **X** near the 5′-end or with a pyrimidine flanking on the 3′-side (Table 1, **ON3**:**DNA** and **ON6**:**DNA**, respectively). Significantly smaller increases, or even minor decreases in duplex stability, are observed towards complementary RNA (ΔT_m = −1.0 to +6.0 °C, Table 1). Similar effects have been observed for 2′-*O*-pyrenylmethyl uridine derivatives, although with significantly less pronounced increases in duplex stability.[20] The Watson–Crick selectivity of monomer **X** was evaluated by determining thermal denaturation temperatures of duplexes formed between **ON4** and DNA or RNA strands containing a single mismatched nucleotide opposite of monomer **X** (Table 1; footnotes c and d). The base pairing selectivity of monomer **X** was satisfactory for T:C DNA and RNA mismatches (−12.5 °C/−12.0 °C, respectively), whereas only a relatively weak decrease in thermal stability was observed for the T:G and T:T/U mismatches. Altogether, the substantial DNA selectivity, limited mismatch discrimination and red-shifts of pyrene absorption maxima upon hybridization of **ON3**–**ON7** to complementary DNA or RNA (Table S1†),[21] indicate that the pyrene moiety of monomer **X** is intercalating upon hybridization.

Next, duplexes involving two strands, each containing one monomer **X**, were studied. Positioning of two monomers **X** in +4, −3 or −1 interstrand zipper arrangements (Table 2, see schematic

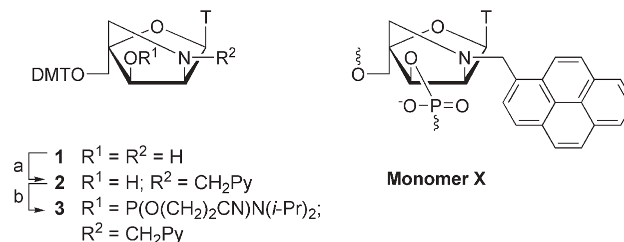

Scheme 1 Synthesis of phosphoramidite **3** and structure of monomer **X**.† *Reagents and conditions:* a) pyrene-1-carbaldehyde, $NaBH(OAc)_3$, $ClCH_2CH_2Cl$, rt, 67%; b) $NC(CH_2)_2OP(Cl)N(i\text{-}Pr)_2$, *N*,*N*-diisopropylethylamine, CH_2Cl_2, rt, 88%. T = thymin-1-yl, Py = pyren-1-yl.

Table 1 Thermal denaturation data for **ON1**–**ON7** towards DNA and RNA complements[a]

		T_m [ΔT_m] (°C)	
		DNA[b]	RNA
ON1	5′-GTG ATA TGC	28.0	26.0
ON2	3′-CAC TAT ACG	28.0	24.5
ON3	5′-G**X**G ATA TGC	35.5 [+7.5]	27.0 [+1.0]
ON4	5′-GTG A**X**A TGC	42.5 [+14.5][c]	31.5 [+5.5][d]
ON5	5′-GTG ATA **X**GC	39.0 [+11.0]	28.0 [+2.0]
ON6	3′-CAC **X**AT ACG	35.0 [+7.0]	23.5 [−1.0]
ON7	3′-CAC TA**X** ACG	44.0 [+16.0]	32.0 [+6.0]

[a] Thermal denaturation temperatures [T_m values (°C) (ΔT_m = change in T_m value calculated relative to DNA:DNA or DNA:RNA reference duplex)] measured as the maximum of the first derivative of the melting curve (A_{260} *vs.* temperature) recorded in medium salt buffer ([Na^+] =110 mM, [Cl^-] =100 mM, pH 7.0 (NaH_2PO_4/Na_2HPO_4)), using 1.0 μM concentrations of the two complementary strands. T_m values are averages of at least two measurements; see Scheme 1 for structure of monomer **X**. MALDI-MS *m/z* ([M − H]$^-$; found/calc.): **ON3**, 2993/2994; **ON4**, 2992/2994; **ON5**, 2994/2994; **ON6**, 2921/2923; **ON7**, 2922/2923. [b] **ON1** is the complementary DNA strand to **ON2/ON6/ON7**; **ON2** is the complementary DNA strand to **ON1/ON3/ON4/ON5**. [c] T_m values (°C) towards DNA strands containing a single mismatch in the central position C/G/T: 30.0/37.0/39.0. [d] T_m values (°C) towards RNA strands containing a single mismatch in the central position C/G/U: 19.5/30.5/27.0.

Table 2 Thermal denaturation data, fluorescence properties and schematic illustrations of duplexes with 2′-amino-α-L-LNA monomer **X** positioned in various interstrand zipper motifs[a]

Duplex	T_m [ΔT_m/mod] (°C)	Excimer	Schematic illustration	Constitution
ON3:**ON7**	53.5 [+12.8]	—	5′ 3′	+4 Zipper
ON3:**ON6**	28.5 [+0.3]	Weak	5′ 3′	+2 Zipper
ON4:**ON7**	31.0 [+1.5]	Strong	5′ 3′	+1 Zipper
ON4:**ON6**	44.0 [+8.0]	—	5′ 3′	−1 Zipper
ON5:**ON7**	46.5 [+9.3]	—	5′ 3′	−1 Zipper
ON5:**ON6**	46.5 [+9.3]	—	5′ 3′	−3 Zipper

[a] For conditions of thermal denaturation experiments, see Table 1. The black droplets illustrate the pyrene moieties of **X** monomers.

illustrations) results in approximately additive increases in thermal stability, whereas only very weak increases, relative to unmodified reference duplexes, were observed for +1 or +2 interstrand zipper arrangements of monomer **X**.§

The distinctive character of +1 or +2 interstrand zipper arrangements of monomers **X** is also reflected in their steady-state fluorescence emission spectra.† The emission spectra of duplexes with monomers **X** in +4, −1 or −3 zipper arrangements (using an excitation wavelength of 340 nm) display relatively weak but structured pyrene monomer bands at λ_{max} ~378 nm and ~396 nm, whereas an additional weak unstructured band at λ_{max} ~430–530 nm (typical region for pyrene–pyrene excimer bands)[22–24] is observed for the +2 zipper motif (Fig. 1). A very intense excimer band as well as a large general increase in fluorescence intensity is observed for the +1 zipper motif (Fig. 1).

The reasons for the observed differences in thermal stability and directional preferences for interstrand pyrene–pyrene excimer formation are the subject of ongoing structural studies. However, close proximity of the pyrene moieties (~3.4 Å)[22] in the +1 zipper orientation is one structural characteristic evidenced by the pyrene–pyrene excimer formation. Interestingly, the lowest energy structure from molecular modelling studies of **ON4**:**ON7**, initially built with a standard B-type helical geometry and with the pyrene moieties pointing into the major groove, suggests that the spatial separation between the pyrene moieties is too large (shortest distance ~12 Å) to facilitate interstrand pyrene–pyrene excimer formation in the major groove (Fig. S1).† Instead, examination of models suggests that the pyrene moieties are adequately positioned to intercalate between the thymine of monomer **X** and the nucleobase of the 3′-flanking nucleotide. We speculate that it is simultaneous intercalation of both pyrene moieties in **ON4**:**ON7** (Fig. 2) that results a) in stacking of two pyrene moieties, accounting for the excimer formation, and b) in significant unwinding of the duplex, as observed for other ONs modified with intercalating pyrene moieties.[25] Thereby, the distance between pyrene moieties and neighboring nucleobases is increased, accounting for the observed decrease in thermal stability and increase in fluorescence intensity.

The lower thermal stability of the double-stranded +1 zipper probe (**ON4**:**ON7**, Table 2) and the reference dsDNA **ON1**:**ON2**

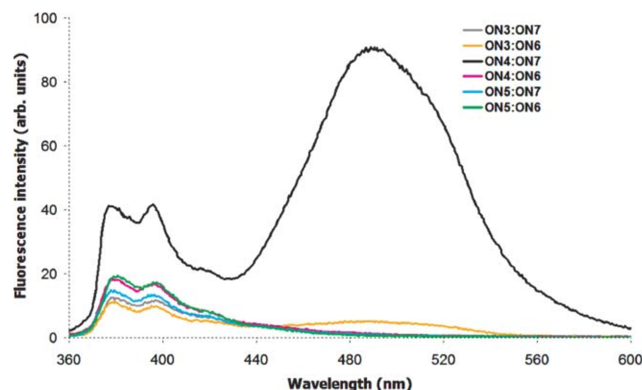

Fig. 1 Steady-state fluorescence emission spectra of DNA duplexes with monomer **X** positioned in various interstrand zipper motifs using an excitation wavelength of 340 nm. Spectra were recorded at 19 °C using 1.0 μM of each strand in thermal denaturation buffer.†

Fig. 2 Schematic illustration of a putative intercalation mode of the pyrene moieties in **ON4**:**ON7**, accounting for excimer band formation.

This journal is © The Royal Society of Chemistry 2005

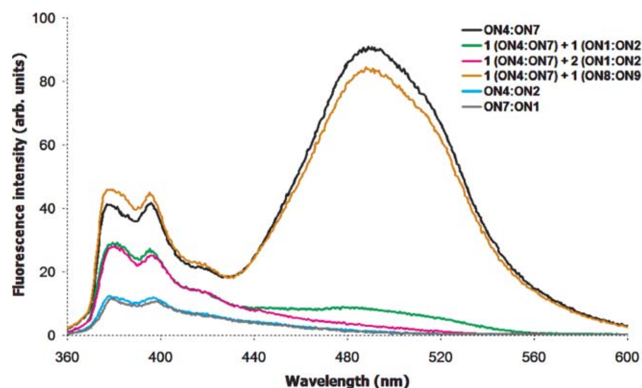

Fig. 3 Steady-state fluorescence emission spectra of molecular recognition experiments using 1 equiv. of the +1 zipper probe (**ON4**:**ON7**) and either 1 or 2 equiv. of fully base-paired unmodified 9-mer dsDNA target **ON1**:**ON2** with an identical sequence as the probe, or 1 equiv. of fully base-paired unmodified 9-mer dsDNA target **ON8**:**ON9** with a sequence differing at two positions from the probe (underlined). **ON8**: 5′-d(GTG GTA CGC)-3′; **ON9**: 5′-d(GCG TAC CAC)-3′.†

as compared to the high-affinity binding of **ON4** and **ON7** to DNA complements (Table 1) suggested that it could be thermodynamically favorable to target the reference dsDNA using the +1 zipper probe **ON4**:**ON7**. Moreover, since the +1 zipper probe exhibits a strong pyrene–pyrene excimer (Fig. 1), whereas there is a complete absence of an excimer band in the fluorescence spectra of the corresponding singly modified ONs against complementary DNA (**ON4**:**ON2** and **ON7**:**ON1**, Fig. 3), fluorescence could be used to monitor any process leading to the dissociation of the +1 zipper probe (such as strand exchange with dsDNA) in solution in real-time. Indeed, addition of pre-annealed double-stranded +1 zipper probe to an equimolar quantity or two-fold excess of pre-annealed complementary 9-mer dsDNA **ON1**:**ON2** in T_m-buffer at 19 °C, *i.e.* below the denaturation temperature of any of the involved duplexes, results in a very fast (<1 min) disappearance of the excimer band and a simultaneous decrease in fluorescence intensity (Fig. 3).§ To verify the fluorescence-based assay and rule out the possibility of non-specific effects, the +1 zipper probe was added to an equimolar quantity of fully base-paired 9-mer dsDNA (**ON8**:**ON9**) containing two mismatched base pairs with respect to the probe. Gratifyingly, the fluorescence emission spectrum of the resulting solution was nearly identical to that observed for the +1 zipper probe alone (Fig. 3) signifying specific targeting of dsDNA.¶||

In conclusion, double-stranded +1 zipper probes of 2′-*N*-(pyren-1-yl)methyl-2′-amino-α-L-LNAs represent a new class of probes for the targeting of dsDNA using a similar strategy as pcDNA[4–6] or pcPNA[6,7] and other potentially dsDNA strand invading probes.[26,27] It is promising that these probes effect efficient molecular recognition of dsDNA targeting mixed sequences at physiologically relevant salt concentrations using a 1:1 ratio between probe and dsDNA. Furthermore, it is noteworthy that the recognition process is fast and that the probe is composed of unmodified DNA strands containing only one pyrene-functionalized 2′-amino-α-L-LNA monomer. The strategy is currently being refined towards realizing a new paradigm for general recognition of longer dsDNA for diagnostic and therapeutic applications.

We greatly appreciate funding from The Danish National Research Foundation.

Notes and references

§ Similar results have been observed in 13-mer mixed sequence contexts (data not shown).

¶ T_m-values of **ON4**:**ON9**, **ON7**:**ON8** and **ON8**:**ON9**, using the conditions described in Table 1, are 17.0 °C, <10 °C and 36.5 °C, respectively.

|| **ON4**:**ON7** was also added to an equimolar quantity of fully base-paired 9-mer dsDNA targets (**ON10**:**ON11**, **ON12**:**ON13** or **ON14**:**ON15**) containing one mismatched base pair with respect to the probe (Fig. S2).† Larger decreases in excimer intensity are observed, reflecting the relatively weak decrease in thermal stability observed for **ON4** with single mismatched DNA-targets (Table 1; footnote c).

1 P. B. Dervan, *Bioorg. Med. Chem.*, 2001, **9**, 2215.
2 S. Buchini and C. J. Leumann, *Curr. Opin. Chem. Biol.*, 2003, **7**, 717.
3 V. V. Demidov, *Expert Rev. Mol. Diagn.*, 2001, **1**, 343.
4 I. V. Kutyavin, R. L. Rhinehart, E. A. Lukhtanov, V. V. Gorn, Jr., R. B. Meyer, Jr. and H. B. Gamper, *Biochemistry*, 1996, **35**, 11170.
5 J. Woo, R. B. Meyer, Jr. and H. B. Gamper, *Nucleic Acids Res.*, 1996, **24**, 2470.
6 I. V. Smolina and V. V. Demidov, *Chem. Biol.*, 2003, **10**, 591.
7 J. Lohse, O. Dahl and P. E. Nielsen, *Proc. Natl. Acad. Sci. USA*, 1999, **96**, 11804.
8 K. I. Izvolsky, V. V. Demidov, P. E. Nielsen and M. Frank-Kamenetskii, *Biochemistry*, 2000, **39**, 10908.
9 V. V. Demidov, E. Protozanova, K. I. Izvolsky, C. Price, P. E. Nielsen and M. D. Frank-Kamenetskii, *Proc. Natl. Acad. Sci. USA*, 2002, **99**, 5953.
10 S. K. Singh, P. Nielsen, A. A. Koshkin and J. Wengel, *Chem. Commun.*, 1998, **63**, 455.
11 S. Obika, D. Nanbu, Y. Hari, J. Andoh, K. Morio, T. Doi and T. Imanishi, *Tetrahedron Lett.*, 1998, **39**, 5401.
12 J. Wengel, *Acc. Chem. Res.*, 1999, **32**, 301.
13 S. K. Singh, R. Kumar and J. Wengel, *J. Org. Chem.*, 1998, **63**, 10035.
14 M. D. Sørensen, L. Kværnø, T. Bryld, A. E. Håkansson, B. Verbeure, G. Gaubert, P. Herdewijn and J. Wengel, *J. Am. Chem. Soc.*, 2002, **124**, 2164.
15 M. D. Sørensen, M. Petersen and J. Wengel, *Chem. Commun.*, 2003, 2130.
16 P. J. Hrdlicka, B. R. Babu, M. D. Sørensen and J. Wengel, *Chem. Commun.*, 2004, 1478.
17 B. R. Babu, P. J. Hrdlicka, C. J. McKenzie and J. Wengel, *Chem. Commun.*, 2005, 1705.
18 J. Wengel, *Org. Biomol. Chem.*, 2004, **2**, 277.
19 We define a 2′-amino-α-L-LNA as an oligonucleotide containing one or more 2′-amino-2′-deoxy-2′-*N*,4′-*C*-methylene-α-L-ribofuranosyl monomer(s).
20 K. Yamana, R. Iwase, S. Furutani, H. Tsuchida, H. Zako, T. Yamaoka and A. Murakami, *Nucleic Acids Res.*, 1999, **27**, 2387.
21 Red shifts of pyrene absorption maxima upon hybridization have previously been used to substantiate intercalation of pyrene moieties. See: A. Okamoto, T. Ichiba and I. Saito, *J. Am. Chem. Soc.*, 2004, **126**, 8364.
22 J. B. Birks, *Acta Phys. Pol.*, 1968, **34**, 603.
23 Interstrand excimer formation in the major groove has been observed for a +2 zipper arrangement of pyrenylmethyl *ara*-uridine-2′-carbamates, although significantly less stable duplexes were formed: N. N. Dioubankova, A. D. Malakhov, D. A. Stetsenko, M. J. Gait, P. E. Volynsky, R. G. Efremov and V. A. Korshun, *ChemBioChem*, 2003, **4**, 841.
24 In general, a broad structureless band at λ = 430–530 nm is attributed to the pyrene–pyrene excimer formation; see *e.g.* A. Mahara, R. Iwase, T. Sakamoto, K. Yamana, T. Yamaoka and A. Murakami, *Angew. Chem. Int. Ed.*, 2002, **41**, 3648.
25 C. B. Nielsen, M. Petersen, E. B. Petersen, P. E. Hansen and U. B. Christensen, *Bioconjugate Chem.*, 2004, **15**, 260.
26 T. Bryld, T. Højland and J. Wengel, *Chem. Commun.*, 2004, 1064.
27 V. V. Filichev, U. B. Christensen, E. B. Pedersen, B. R. Babu and J. Wengel, *ChemBioChem*, 2004, **5**, 1673.

This journal is © The Royal Society of Chemistry 2005